

Infrared Observations of the Jovian System from Voyager 2

Abstract. *Infrared spectra obtained from Voyager 2 have provided additional data on the Jovian system, complementing those obtained from Voyager 1. The abundance ratio of ethane to acetylene in Jupiter's atmosphere appears to be about three times larger in the polar regions than at lower latitudes. A decidedly hemispherical asymmetry exists, with somewhat higher ratios prevailing in northern latitudes. An overall increase in the abundance ratio by a factor of about 1.7 appears to have occurred between the Voyager 1 and 2 encounters. Global brightness temperature maps of Jupiter at 226 and 602 cm^{-1} exhibit a large amount of local- and planetary-scale structure, as well as temporal variability. Although heterogeneous cloud structure and ammonia concentration in the lower troposphere may contribute to the appearance of the 226- cm^{-1} map, the detail in the 602- cm^{-1} maps probably represents the actual horizontal thermal structure near the tropopause and suggests that dynamical heating and cooling processes are important. Low-latitude surface temperatures on the Galilean satellites range from approximately 80 K on the dark sides to 155 K at the subsolar point on Callisto. Below a thin insulating layer, the thermal inertia of Callisto is somewhat greater than that of Earth's moon. Upper limits on the infrared optical depth of the Jovian ring ranging from approximately 3×10^{-4} at 250 cm^{-1} to 3×10^{-3} at 600 cm^{-1} have been found.*

The infrared spectroscopy and radiometry (IRIS) instrument on Voyager 2 is identical to the one on Voyager 1 (1). It consists of a Michelson interferometer for the infrared (180 to 2500 cm^{-1}) with a spectral resolution of 4.3 cm^{-1} , and a radiometer for the visible and near infrared (5000 to 25,000 cm^{-1}). Both devices share a 50-cm Cassegrain telescope with a field of view 0.25° in diameter. A small misalignment of the interferometer on Voyager 1 was also present and even slightly more pronounced on Voyager 2; this resulted in a lower responsivity and consequently a higher noise equivalent spectral radiance in the Voyager 2 instrument. For example, at 2000 cm^{-1} the responsivity of the Voyager 2 IRIS apparatus was about half that of Voyager 1, whereas at low wave numbers, the instruments on the two spacecraft per-

formed nearly alike. The response of the Voyager 2 IRIS changed gradually with time during the encounter period. In the final calibration, this temporal effect, though small, will be removed. Since this has not yet been done, the data shown in this report must be considered preliminary.

As on Voyager 1, the Voyager 2 instrument returned a large number of spectral and radiometric data on Jupiter and its satellites for varying conditions of latitude, longitude, local time, and phase and emission angles. Spectra of Jupiter from both spacecraft are shown in Figs. 1 and 2. In each case, 133 near-encounter spectra with brightness temperatures greater than 240 K at 2000 cm^{-1} were averaged. As expected, the spectra are nearly identical, with minor differences attributable to the temporal and spatial

differences between the data sets. Consistent with the measured responsivities, the Voyager 2 average spectrum is slightly noisier than that from Voyager 1. The purpose of this report is to show selected examples of results from the Voyager 2 infrared investigation.

Latitudinal variation of the abundance ratio of ethane to acetylene. Upon comparing Voyager 1 high- and low-latitude data at comparable emission angles, it became evident that the intensity of the ν_9 C_2H_6 band at 821 cm^{-1} tended to increase with increasing latitude relative to that of the ν_5 C_2H_2 band at 729 cm^{-1} . Further analysis demonstrated that this effect could not be due solely to thermal structure differences, but that the observed relative intensities were directly related to differences in the abundance of the two hydrocarbons. Since the actual latitudinal distribution of abundances depends on the relative importance of various stratospheric photochemical and dynamical transport processes, an observational determination of this distribution provides a useful discriminant in assessing the relative merits of different theoretical stratospheric models.

Unfortunately, the spatial resolution in the Voyager 1 data set was insufficient for adequately characterizing the latitudinal distribution of hydrocarbons near the poles; only gross averages could be obtained for each polar region. In consequence, a change in the Voyager 2 observational sequence was made in order to attain higher spatial resolution near the poles. The successful implementation of this change has allowed completion of the overall data set needed for an adequate analysis.

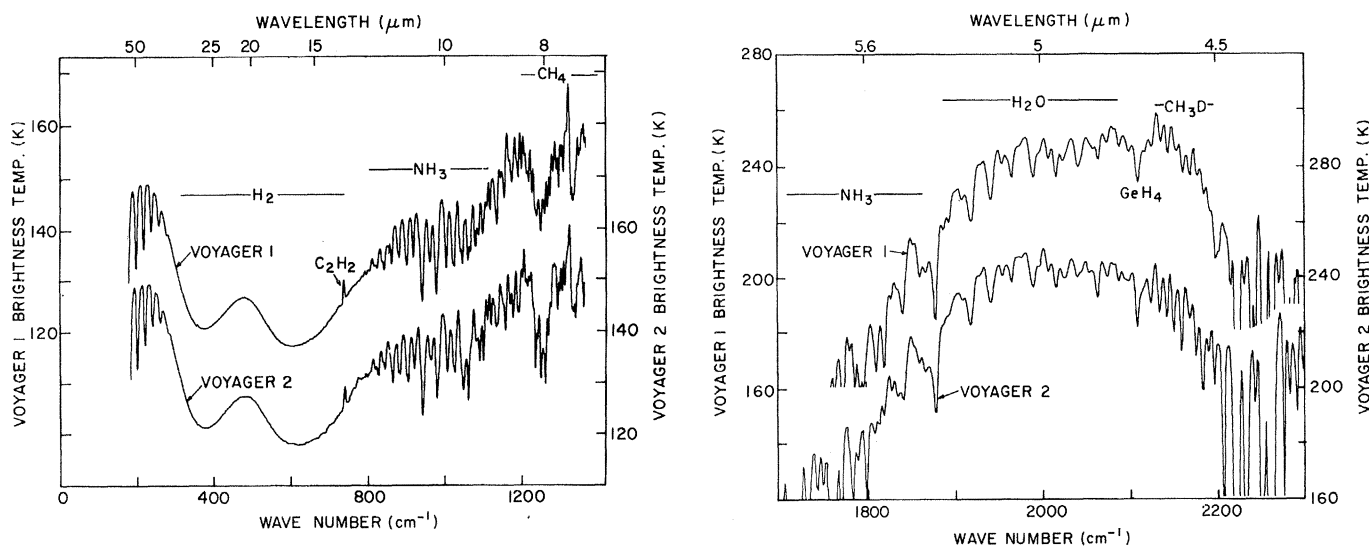


Fig. 1 (left). Thermal emission spectra for Voyager 1 and 2. Strong spectral features are seen for the gases H_2 , C_2H_2 , NH_3 , and CH_4 . Significant PH_3 absorption occurs in the region between 1100 and 1200 cm^{-1} , the strongest feature being the Q branch at 1122 cm^{-1} . Fig. 2 (right). Thermal emission spectra in the 2000- cm^{-1} Jovian window for Voyager 1 and Voyager 2. Strong absorption features of NH_3 , H_2O , GeH_4 , and CH_3D are seen.

The $C_2H_6(\nu_9) : C_2H_2(\nu_5)$ ratio of band intensities is shown as a function of latitude for each spacecraft in Table 1. All measurements were taken near the limb at roughly comparable emission angles. Because no significant diurnal variation was found, we averaged the data without regard to longitude or local hour angle.

A definite asymmetry appears superimposed on the overall latitudinal dependence of band intensity ratios, with the larger values tending to favor the northern hemisphere. Although the ratios obtained from Voyager 1 show a latitudinal dependence similar to those of Voyager 2, they are systematically smaller by about a factor of 1.7. The contributions to this difference from calibration and signal-to-noise differences between the two instruments should be small. Because of the intrinsically higher spatial resolution of the Voyager 2 polar observations, the emission angles appropriate to the polar limb data are somewhat larger than those for Voyager 1. The empirical determination that the $C_2H_6 : C_2H_2$ ratio of band intensities increases with increasing emission angle suggests that a small part of the apparent discrepancy can be removed by properly accounting for the difference in angles. The disparity at lower latitudes remains unaffected. In any event, only a minor fraction of the difference between the two spacecraft data sets can be ascribed to instrumental or observational selection effects, which implies that a real change in the Jovian atmosphere has occurred between the two encounters.

The most dramatic variation of the band intensity ratio with latitude is indicated by the Voyager 2 data in the south polar region. The relevant averaged spectra (Fig. 3) demonstrate that variations with local time or longitude are small compared with those dependent on latitude. The major effect seems to be the tendency toward depletion of C_2H_2 with increasing latitude. However, it is not yet possible to draw firm conclusions regarding the latitudinal distribution of C_2H_2 because the different vertical temperature structures at different locations on the disk of Jupiter have not yet been included in the analysis. Comparable conclusions regarding the $C_2H_6 : C_2H_2$ abundance ratio do not depend nearly so strongly on the actual temperature profiles; hence the abundance ratios should mimic the corresponding band intensity ratios rather closely. Once the quantitative modeling now being carried out is completed, more definitive statements about the latitudinal dependence of individual abundances can be made.

Table 1. Ratios of band intensities $C_2H_6(821\text{ cm}^{-1}):C_2H_2(729\text{ cm}^{-1})$. The total outgoing energy radiated in each band relative to the adjacent continuum is calculated, and the ratios taken. All data for a given spacecraft correspond to roughly equivalent high-emission angles near the limb. Owing to the basically lower spatial resolution, Voyager 1 polar data are generally integrated over a larger and lower emission-angle range than are the Voyager 2 polar data.

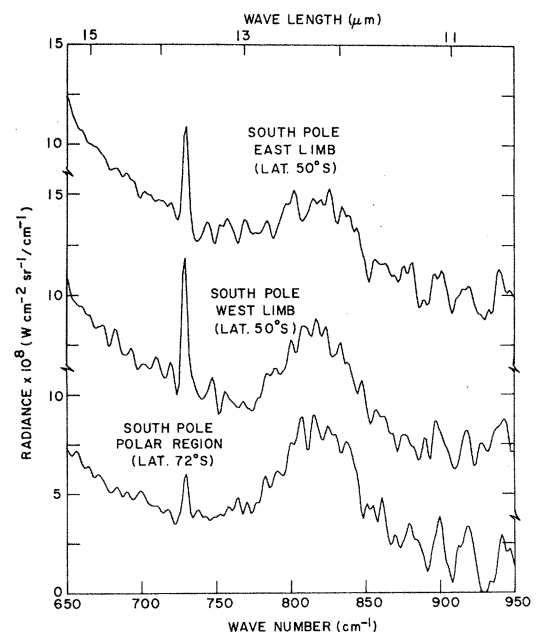
Region	Voyager 2			Voyager 1		
	Latitude	Band ratio	Effective emission angle (degrees)	Latitude	Band ratio	Effective emission angle (degrees)
North polar	58°N	35	72	57°N	17	53
	48°N	27	68			
Zone	27°N	15	60	24°N	9.4	60
Belt	12°N	10	58	12°N	6.1	62
South polar	50°S	10	67	59°S	11	58
	72°S	37	68			

Atmospheric thermal structure. The Voyager IRIS spectra provide extensive information on the thermal structure of the Jovian atmosphere. The Voyager 1 IRIS report (1) presented vertical cross sections of temperature derived by inversion of spectral data. Of equal interest are horizontal structure and time variability. In this report, a preliminary examination of these aspects of the atmospheric temperature field is carried out through the use of global brightness temperatures at selected wave numbers.

Maps of brightness temperature at 226 cm^{-1} and 602 cm^{-1} , constructed from Voyager 2 data taken approximately 3 days before encounter, are shown in Figs. 4 and 5. The data were acquired during one rotation of the planet and from north-south scans passing through the subspacecraft point. The spatial resolution near the equator is approximately 8° of latitude and longitude. At normal viewing, the maximum contribution to the thermal emission at 226 cm^{-1} occurs

at about 800 mbar. This wave-number interval lies in a continuum between two NH_3 lines and is in the most transparent part of the long-wave portion of the spectrum. Brightness temperatures in this region may respond to the presence of clouds as well as variations in the NH_3 abundance and the thermal structure of the lower troposphere. The weighting function describing the relative contribution of each level to the outgoing radiation at 602 cm^{-1} peaks near 150 mbar (approximately the tropopause level) with half-amplitude points at 50 and 300 mbar; thus, brightness temperatures in this spectral region reflect the behavior of the thermal structure in the upper troposphere and lower stratosphere. Small effects due to hazes could be present in both maps, although a preliminary examination of the data indicates none of the obvious spectral signatures expected for NH_3 particles. The maps shown have not been corrected for varying emission angle; therefore, limb darkening is evi-

Fig. 3. Voyager 2 high-emission-angle (limb) radiance spectra of the south polar region. The spectra are averages of 19, 12, and 18 individual spectra of the east limb, west limb, and polar region, respectively. The Q branch of the ν_5 band of C_2H_2 peaks sharply at 729 cm^{-1} while the broad ν_9 band of C_2H_6 is centered at 821 cm^{-1} . Although the data are somewhat noisy, the larger absorption features in the 850 to 950 cm^{-1} region are real and attributable to NH_3 located primarily in the troposphere. The hydrocarbon bands are seen in emission and are principally stratospheric in origin.



dent with increasing latitude at 226 cm^{-1} while moderate limb brightening can be observed at 602 cm^{-1} .

The gross belt-zone structure observed in visual imaging is apparent in the thermal maps. Relatively cold regions occur in both maps at approximately 20° to 35°N and 20° to 35°S , corre-

sponding to bright zones seen in Voyager images. The warmest temperatures in both maps occur between approximately 15°N and 15°S , which is associated with a visually dark equatorial belt.

Perhaps the most striking aspect of the maps is the abundance of relatively localized features. In some cases, these

areas can be correlated with visual features seen in the Voyager images. For example, the cold area observed at 602 cm^{-1} near 23°S , 105°W is associated with the Great Red Spot, and the warm feature near 13°N , 215°W coincides with one of the dark brown elongated spots discussed by Smith *et al.* (2). On the oth-

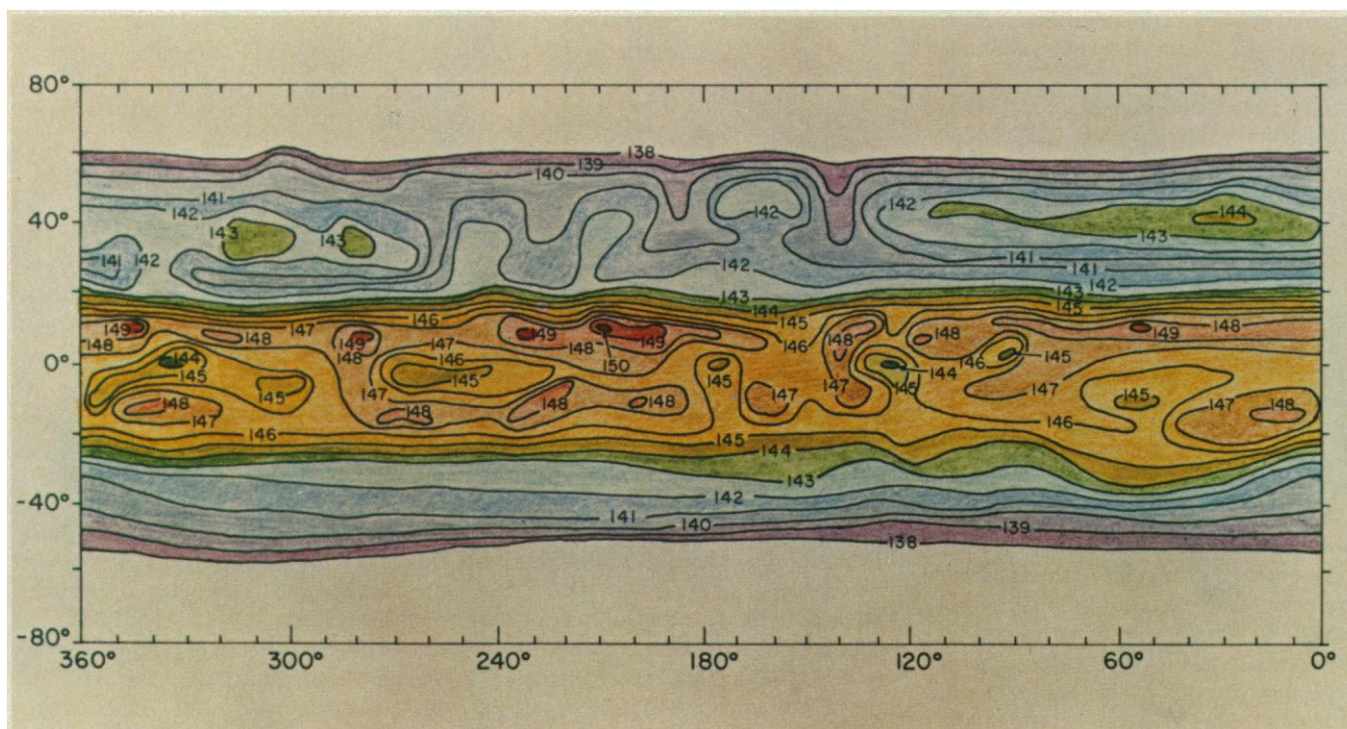


Fig. 4. Voyager 2 brightness temperature map of Jupiter at 226 cm^{-1} . At normal viewing of a clear atmosphere, this corresponds to a pressure of approximately 800 mbar. The ordinate and abscissa are latitude and west longitude, respectively. Temperature contours are labeled in degrees Kelvin.

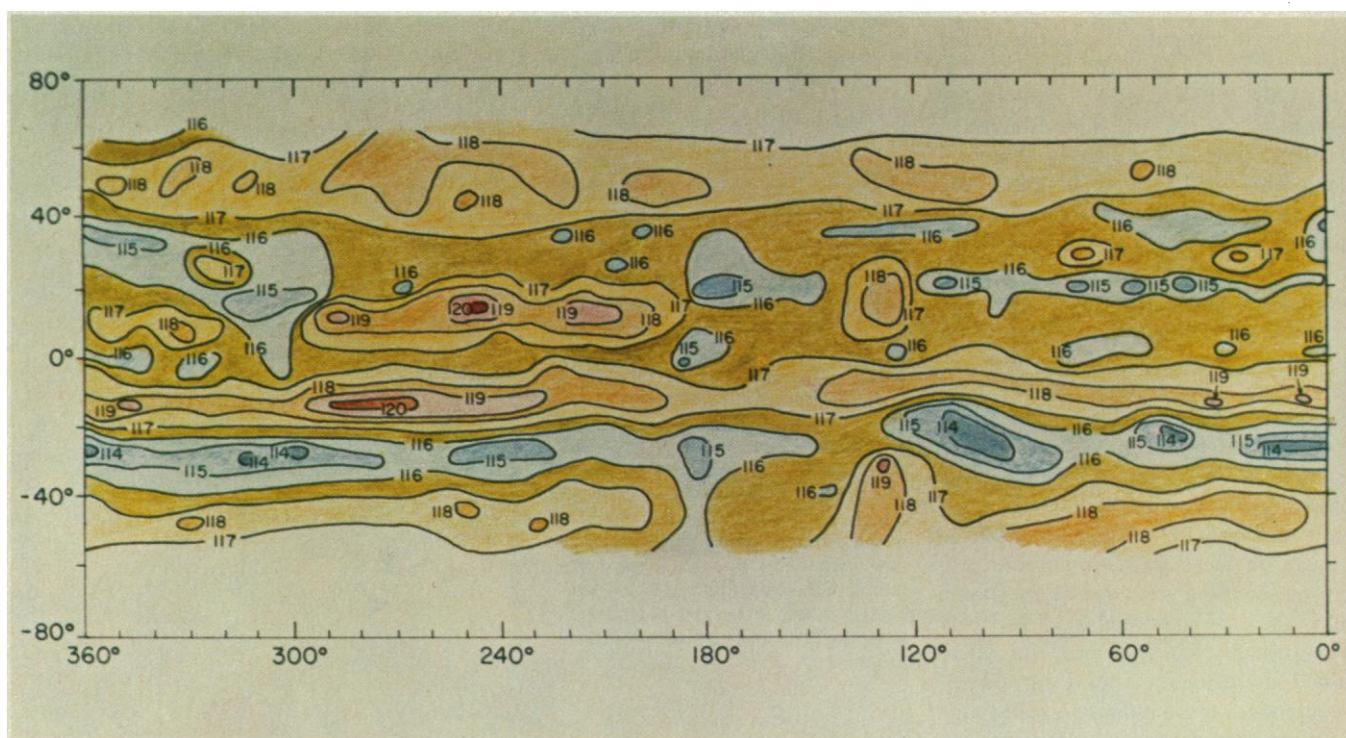


Fig. 5. Voyager 2 brightness temperature map of Jupiter at 602 cm^{-1} , corresponding to a pressure of 150 mbar. The map is labeled as in Fig. 4.

er hand, many other thermal variations are not obviously correlated with visual features. Comparison of localized features in the 602-cm⁻¹ map with those at 226 cm⁻¹ is also of interest. Warm features within the equatorial belt in both maps correlate rather well. Other features, however, do not. For example, the Great Red Spot is not very apparent at 226 cm⁻¹.

The reasons for the local variations in brightness temperatures are not yet fully understood. The 602-cm⁻¹ temperatures are most likely reflecting true atmospheric temperature differences in the vicinity of the tropopause. In some cases these temperature differences may be caused by adiabatic heating and cooling resulting from localized forced vertical motion. Other possible causes include horizontal advective transport and local radiative effects associated with clouds or hazes. Because of the depth from which the 226-cm⁻¹ radiation would originate in a clear atmosphere, the brightness temperatures at this frequency should be more sensitive to clouds. Although there appears to be a correlation with gross cloud structure, an examination of Fig. 4 suggests that when limb darkening is taken into consideration, any cloud decks that are completely opaque at this frequency must lie below the 140 K level (~ 500 mbar). Although the spectral interval lies between NH₃ lines, there is still significant NH₃ absorption, and variations in ammonia abundance may affect these measurements.

Table 2. Upper limit to normal optical depth of the Jovian ring; $I(\nu)$ is the upper limit of signal in the infrared spectrum of the ring.

ν (cm ⁻¹)	$I(\nu)$ (W cm ⁻² sr ⁻¹ /cm ⁻¹)	$\tau(\nu)$
250	1×10^{-9}	3×10^{-4}
400	1×10^{-9}	5×10^{-4}
600	2×10^{-9}	3×10^{-3}

To obtain some estimate of possible temporal variations, a map at 602 cm⁻¹ at comparable spatial resolution was constructed from Voyager 1 data acquired approximately 4 months earlier (Fig. 6). The Voyager 1 and 2 maps are similar in their gross features; however, the Voyager 2 data appear to be systematically warmer by approximately 1 K, probably as a result of errors in the preliminary Voyager 2 calibration. Anticipated changes in the longitude of specific features such as the Great Red Spot are evident, but there also appear to be significant intrinsic changes in certain areas such as the localized warm features slightly south of the equator. The occurrence of such changes over a time scale of a few months suggests they are related to dynamic processes, since the radiative time constant at this level is of the order of several years.

Jupiter's ring. A set of 20 spectra was obtained during a radial scan of the ring. An average of this set, which showed no evident thermal signal, can be used to set an upper limit on the normal optical

depth of the ring in the thermal infrared. For an optically thin emitting medium, the normal optical depth $\tau(\nu)$ is given by

$$\tau(\nu) = I(\nu) [f \sec \theta B(\nu, T)]^{-1}$$

where $I(\nu)$ is the measured signal strength at wave number ν , f is the fraction of the instrument field of view filled by the medium, θ is the view angle measured from the normal, and B is the Planck function at the ring temperature T . From images taken during the observational sequence (3), the bright portion of the ring in the IRIS field of view gives $f = 0.088$; the viewing geometry gives $\theta = 88.2^\circ$; an isothermal black ring particle in thermal equilibrium with Jupiter and the sun will have a temperature of about 125 K. By using the instrument noise level as an upper limit to the ring signal, we obtain the upper limit ring opacities (Table 2).

Satellites. Thermal anomalies have previously been observed on Io (1, 3). Seven hours of nearly continuous observations from Voyager 2, obtained during a search for variability in volcanic plumes (4), provide a data base to continue the search for such hot areas. During these observations, Io filled half of the IRIS field of view, so only disk-integrated data were obtained; the longitude of the spacecraft point gradually moved from 10° to 28°W during this time. The observability of "hot spots" is limited by the instrument noise and the thermal contrast between the hot spot and the overall background. In the present

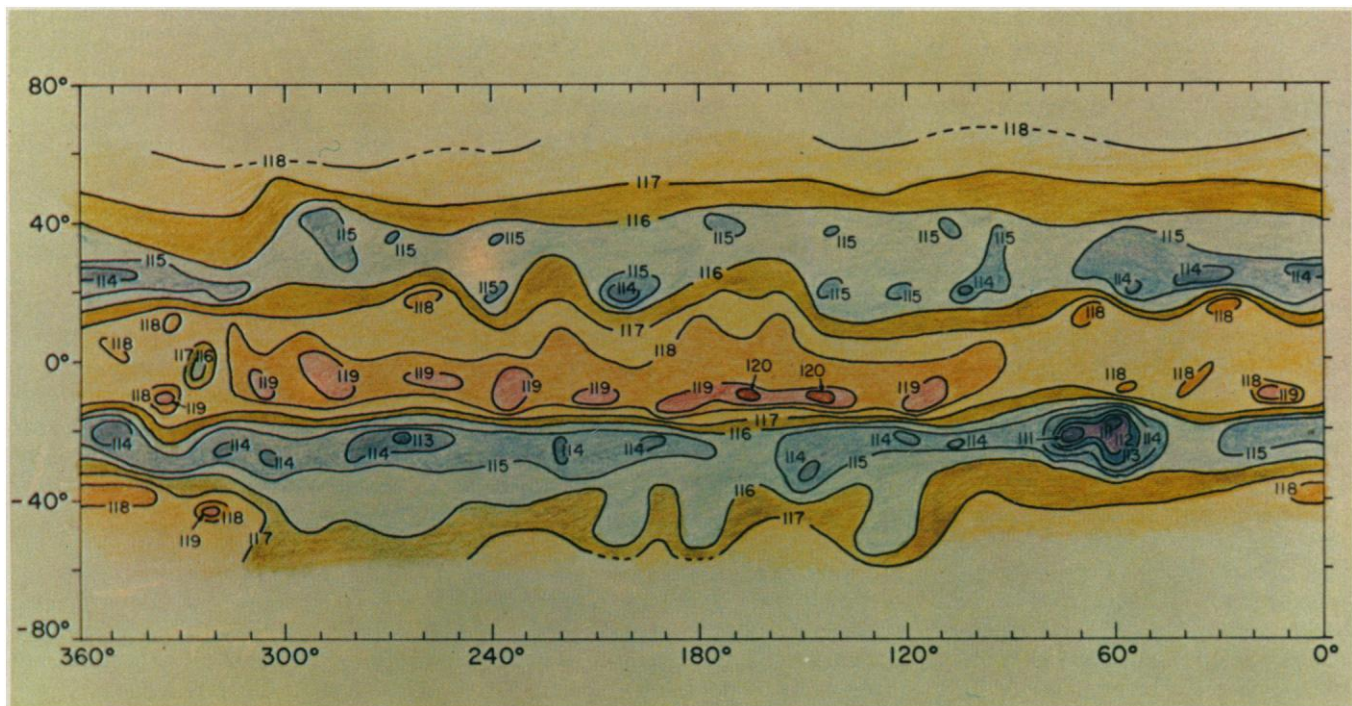


Fig. 6. Voyager 1 brightness temperature map of Jupiter at 602 cm⁻¹, corresponding to a pressure of 150 mbar. The map is labeled as in Fig. 4.

case, the background signal is the radiance arising from diurnal surface heating, integrated over the spacecraft-facing hemisphere. Although thermal data are available from Voyager 1 for various portions of the surface, a comprehensive surface temperature model is not yet complete. A conservative estimate of the ability to detect thermal anomalies can be made, however; viewed at emission angle θ , a circular source should be detectable at, say, 650 cm^{-1} if

$$R^2 B(T) \cos \theta \geq 0.08$$

where R is the source radius (in kilometers) and $B(T)$ is the Planck function ($\text{W cm}^{-2} \text{sr}^{-1} \text{cm}^{-1}$) at temperature T (in degrees kelvin). Thus a thermal event of the magnitude observed by Witteborn *et al.* (3), which could be interpreted as an area 52 km in radius at 600 K, would have been observable from the spacecraft if present on the satellite at a view angle of less than 70° . An area 100 km in radius at 290 K, such as that observed from Voyager 1 (1), would have been observable if at a view angle less than 54° . That no such anomalies were seen limits the thermal emission from the source of plume 8 (5), which was near an emission angle of 45° during the Voyager 2 observations. For example, an exposed area of molten sulfur (385 K) could be no more than 50 km in radius. Further analysis will refine the detection limit and will also enable limits to be placed on the activity associated with plumes 2 and 5, which were very near the limb at this time.

The flyby of Europa provided IRIS spatial resolution of only about one-third of the disk. Limited coverage (15 to 21 hours local time) of the diurnal thermal cycle of the surface was therefore obtained. Surface temperatures between 0° and -40° latitude ranged between 85 and 110 K. This range is consistent with a diurnal maximum equatorial temperature of $\sim 125 \text{ K}$.

Although covering a different hemisphere, the Voyager 2 flyby of Ganymede observed a range of local times similar to that obtained during the Voyager 1 flyby (11 to 24 hours local time). Surface temperatures at low latitudes ranged between 85 and 145 K. A slight wave-number dependence of brightness temperature (approximately 5 K higher at 600 cm^{-1} than at 250 cm^{-1}) is observed. This is generally consistent with the presence of a range of surface temperatures within the instrument field of view, as might be caused by variations in surface albedo and thermal inertia.

The Voyager 2 flyby of Callisto provided the only dawn terminator coverage

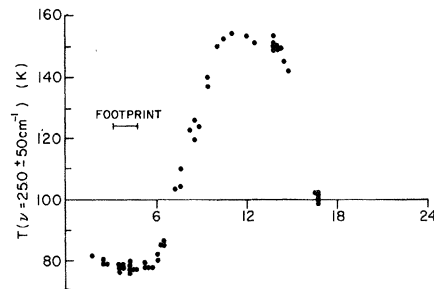


Fig. 7. Brightness temperatures at 250 cm^{-1} versus local time for Callisto. Preenoon data are from Voyager 2; afternoon data are from Voyager 1. Measurements were taken from latitudes between -10° and $+25^\circ$. The approximate range of local time covered by the instrument footprint is indicated. Pointing uncertainties of ± 1 hour in local time may exist.

of a satellite. A plot of low-latitude brightness temperatures at 250 cm^{-1} is shown in Fig. 7. The predawn cooling portion of the curve can be used to estimate the thermal inertia of the near surface layers. According to a heat conduction model with physical properties independent of depth, diurnal heating calculations imply a value of $\sim 2 \times 10^{-3} \text{ cal cm}^{-2} \text{ K}^{-1} \text{ sec}^{-1/2}$. This is about twice as high as the value for Earth's moon obtained under similar assumptions. The comparison suggests that Callisto has a more consolidated subsurface than has Earth's moon, as might be expected if refusion of icy material occurs. The assumption of vertically homogeneous properties is actually invalid; eclipse observations of Callisto indicate a surface layer approximately 1 mm thick with a thermal inertia of $\sim 2 \times 10^{-4} \text{ cal cm}^{-2} \text{ K}^{-1} \text{ sec}^{-1/2}$ overlying a higher inertia layer (6). The present result is consistent with this. Not surprisingly, the daytime behavior of the surface temperatures in Fig. 7 is not well described by the homogeneous model. While the morning warming behavior can be fit with such a

model, the afternoon cooling is too rapid. An additional complication is also introduced by a variation in the wave-number dependence of the brightness temperature with local time. Preliminary attempts to model this behavior with two surface components of different albedos have not been successful. More sophisticated modeling is under way.

R. HANEL, B. CONRATH
M. FLASAR, L. HERATH
V. KUNDE, P. LOWMAN
W. MAGUIRE, J. PEARL

J. PIRRAGLIA, R. SAMUELSON
*Goddard Space Flight Center,
Greenbelt, Maryland 20771*

D. GAUTIER
Paris Observatory, Meudon, France

P. GIERASCH
*Cornell University,
Ithaca, New York 14853*

L. HORN, S. KUMAR
*Jet Propulsion Laboratory,
Pasadena, California 91103*

C. PONNAMPERUMA
*University of Maryland,
College Park 20742*

References and Notes

1. R. Hanel *et al.*, *Science* **204**, 972 (1979).
2. B. A. Smith *et al.*, *ibid.*, p. 951.
3. F. C. Witteborn, J. D. Bregman, J. B. Pollack, *ibid.* **203**, 643 (1979).
4. B. A. Smith *et al.*, *ibid.* **206**, 927 (1979).
5. R. G. Strom, R. J. Terrile, H. Masursky, C. Hansen, *Nature (London)*, in press.
6. D. Morrison and D. P. Cruikshank, *Icarus* **18**, 224 (1973).
7. We thank D. Vanous, D. Crosby, and J. Taylor and their colleagues at Texas Instruments, Goddard Space Flight Center, and Jet Propulsion Laboratory (JPL) for preparation of the instrumentation. F. Rockwell, C. Otis, J. Frost, and P. Corbin (Astro Data Systems, Inc.) contributed substantially to the data reduction. T. Burke, E. Miner, and D. Collins (JPL) made substantial contributions. We also thank the imaging team, especially B. Smith, G. Hunt, and R. Terrile for many discussions and for help in the selection of $5\text{-}\mu\text{m}$ "hot spots" for IRIS observations. The support of the Voyager Project staff is also gratefully acknowledged. Portions of the research described in this report were supported by JPL, California Institute of Technology, under NASA contract NAS 7-100.

27 September 1979

Photometric Observations of Jupiter at 2400 Angstroms

Abstract. *The photopolarimeter instrument on Voyager 2 was used to obtain a map of Jupiter at an effective wavelength of 2400 angstroms. Analysis of a typical north-south swath used to make this map shows strong absorption at high latitudes by a molecular or particulate constituent in the Jovian atmosphere. At 65° north latitude, the absorbing constituent extends to altitudes above the 50-millibar pressure level.*

During the approach phase of the Voyager 2 encounter with Jupiter, the photopolarimeter instrument (I) was programmed to obtain intensity measurements every 0.6 second by using a $300\text{-}\text{\AA}$ bandpass filter centered at 2350 \AA . When combined with the solar flux, the ef-

fective wavelength of these observations is 2400 \AA . With the spacecraft a nominal 48 Jupiter radii (R_J) from Jupiter, the subspacecraft point at 4.5° north latitude, the phase angle 17.5° , and the subsolar point at 0° latitude, the scan-platform pointing direction was articulated